Near-Real-Time SSM/I-SSMIS EASE-Grid Daily Global Ice Concentration and Snow Extent, Versions 2 – 5

USER GUIDE

How to Cite These Data

As a condition of using these data, you must include a citation (note that they are version-specific):

V5: Brodzik, M. J. and J. S. Stewart. 2016. *Near-Real-Time SSM/I-SSMIS EASE-Grid Daily Global Ice Concentration and Snow Extent, Version 5*. [Indicate subset used]. Boulder, Colorado USA. NASA National Snow and Ice Data Center Distributed Active Archive Center. https://doi.org/10.5067/3KB2JPLFPK3R. [Date Accessed].

V4: Nolin, A. W., R. Armstrong, and J. Maslanik. 1998. *Near-Real-Time SSM/I-SSMIS EASE-Grid Daily Global Ice Concentration and Snow Extent, Version 4*. [Indicate subset used]. Boulder, Colorado USA. NASA National Snow and Ice Data Center Distributed Active Archive Center. https://doi.org/10.5067/VF7QO90IHZ99. [Date Accessed].

V3: Brodzik, M. J. and J. S. Stewart. 2021. *Near-Real-Time SSM/I-SSMIS EASE-Grid Daily Global Ice Concentration and Snow Extent, Version 3*. [Indicate subset used]. Boulder, Colorado USA. NASA National Snow and Ice Data Center Distributed Active Archive Center. https://doi.org/10.5067/JAQDJKPX0S60. [Date Accessed].

V2: Nolin, A. W., R. Armstrong, and J. Maslanik. 2019. *Near-Real-Time SSM/I EASE-Grid Daily Global Ice Concentration and Snow Extent, Version 2*. [Indicate subset used]. Boulder, Colorado USA. NASA National Snow and Ice Data Center Distributed Active Archive Center. https://doi.org/10.5067/4FSODMDM1WEJ. [Date Accessed].

FOR QUESTIONS ABOUT THESE DATA, CONTACT NSIDC@NSIDC.ORG

FOR CURRENT INFORMATION, VISIT https://nsidc.org/data/NISE

National Snow and Ice Data Center

TABLE OF CONTENTS

1 DATA DESCRIPTION 2
1.1 Parameters 2
1.2 File Information 2
1.2.1 Format 2
1.2.2 File Contents 2
1.2.3 Sample Data 3
1.2.4 Directory Structure 4
1.2.5 Naming Convention 4
1.3 Spatial Information 5
1.3.1 Coverage 5
1.3.2 Resolution 5
1.3.3 Geolocation 5
1.4 Temporal Information 7
1.4.1 Coverage 7
1.4.2 Resolution 7
2 DATA ACQUISITION AND PROCESSING 7
2.1 Background 7
2.2 Instrumentation 8
2.3 Acquisition 8
2.4 Processing 9
2.5 Quality, Errors, and Limitations 9
2.5.1 Quality Control 9
2.5.2 Error Sources 14
2.5.3 Confidence Level/Accuracy Judgment 15
2.5.4 Applications and Limitations 16
3 SOFTWARE AND TOOLS 16
4 VERSION HISTORY 17
5 RELATED DATA SETS 20
6 CONTACTS AND ACKNOWLEDGMENTS 20
7 REFERENCES 20
8 DOCUMENT INFORMATION 21
8.1 Publication Date 21
8.2 Date Last Updated 21

Note: This documentation applies to all major versions of the Near-Real-Time SSM/I-SSMIS EASE-Grid Daily Global Ice Concentration and Snow Extent (NISE) product. Major versions correspond to different Defense Meteorological Satellite Program (DMSP) missions and unique platform / sensor combinations:
NISE Version 2 *data derive from the Special Sensor Microwave Imager (SSM/I) sensor aboard the DMSP-F13 satellite.*
NISE Version 3 *data derive from the Special Sensor Microwave Imager/Sounder (SSMIS) sensor aboard the DMSP-F16 satellite.*
NISE Version 4 *data derive from the Special Sensor Microwave Imager/Sounder (SSMIS) sensor aboard the DMSP-F17 satellite.*
NISE Version 5 *data derive from the Special Sensor Microwave Imager/Sounder (SSMIS) sensor aboard the DMSP-F18 satellite.*

1 DATA DESCRIPTION

1.1 Parameters

The main parameters for this data set are snow extent (the presence or absence of snow) and sea ice concentration (measured as a percentage).

1.2 File Information

1.2.1 Format

Data are provided in HDF-EOS format. HDF-EOS (Hierarchical Data Format - Earth Observing System) is a self-describing file format based on HDF that was developed specifically for distributing and archiving data collected by NASA EOS satellites. For more information, visit the HDF-EOS Tools and Information Center.

Two JPEG browse images, one for the Northern Hemisphere and one for the Southern Hemisphere, are available for each day.

Extensible Markup Language (`.xml`) files with associated metadata are also provided.

1.2.2 File Contents

Daily data are provided in a single HDF-EOS file containing two data fields, extent and age, for both the Northern and Southern Hemispheres (Table 1). Extent and age values are stored as binary arrays of unsigned 1-byte (8-bit) data ranging in value from 0 to 255.

Table 1. HDF-EOS File Descriptions

Data Field	Description	Possible Values
Extent	The snow coverage and sea ice concentration of all pixels in the study areas; coastal pixels are also identified	0: Snow-free land 1-100: Sea ice concentration (%) 101: Permanent ice coverage (Greenland, Antarctica) 102: Not used 103: Pixel has snow 104-251: Not used 252: Coastal pixel (unable to reliably apply microwave algorithms) 253: Pixel suspected of having ice 254: Corner points (undefined) 255: Ocean
Age	The age of the input data relative to the data file; the difference between the day of acquisition for the input data and the day of production for the HDF-EOS file	0-254: age (in days) before the date of the data file 255: fill value for corner points (off-Earth) and undetermined data pixels

1.2.3 Sample Data

Figure 1 and Figure 2 depict data from 03 February 2002 for the Northern and Southern Hemispheres, respectively.

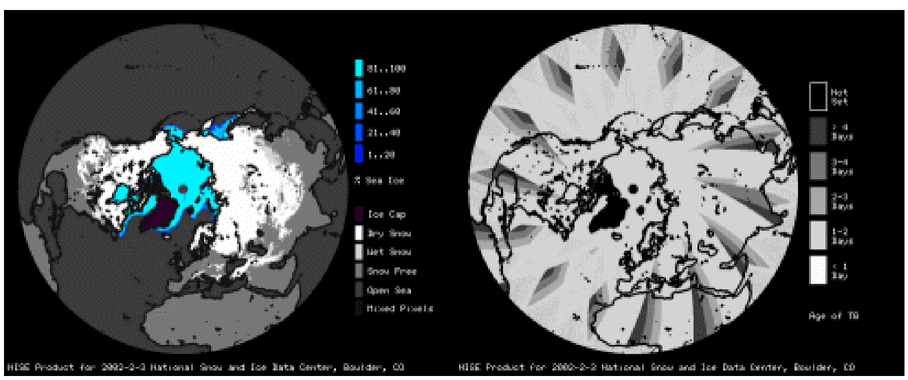

Figure 1. Sample data record for NISE_SSMIF13-20020203_N.GIF.

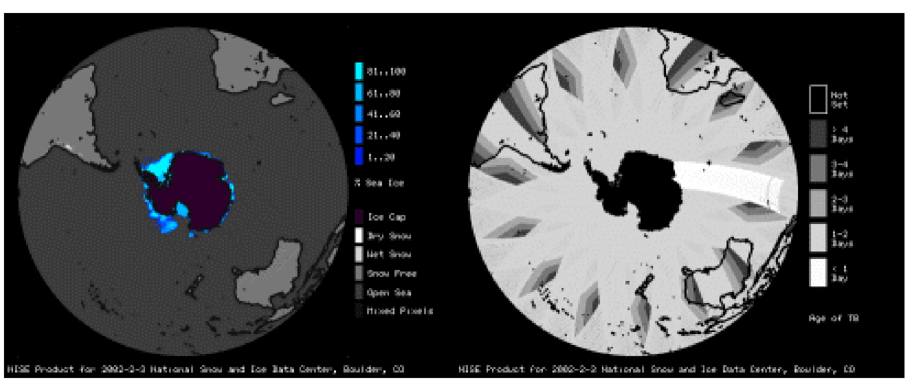

Figure 2. Sample data record for NISE_SSMIF13-20020203_S.GIF.

1.2.4 Directory Structure

NISE Version 2 data can be found at the following location:
https://n5eil01u.ecs.nsidc.org/OTHR/NISE.002/

NISE Version 3 data can be found at the following location:
https://n5eil01u.ecs.nsidc.org/OTHR/NISE.003/

NISE Version 4 data can be found at the following location:
https://n5eil01u.ecs.nsidc.org/OTHR/NISE.004/

NISE Version 5 data can be found at the following location:
https://n5eil01u.ecs.nsidc.org/OTHR/NISE.005/

1.2.5 Naming Convention

Files are named according to the following conventions and as described in Table 2.

```
NISE_SSMIF[##]_yyyymmdd.[h].ext
NISE_SSMISF[##]_yyyymmdd.ext
NISE_SSMISF[##]_yyyymmdd.ext.xml
```

Table 2. Description of File Name Variables

<table>
<tr><th>Variable</th><th>Description</th></tr>
<tr><td>NISE</td><td>Near-real-time Ice and Snow Extent</td></tr>
<tr><td>SSMI(S)</td><td>Special Sensor Microwave Imager(/Sounder): sensor</td></tr>
<tr><td>F##</td><td>DMSP Platform (F13/F16/F17/F18)</td></tr>
<tr><td>yyyy</td><td>4-digit year</td></tr>
<tr><td>mm</td><td>2-digit month of year</td></tr>
<tr><td>dd</td><td>2-digit day of month</td></tr>
<tr><td>h</td><td>Hemisphere (1: Northern, 2: Southern)</td></tr>
<tr><td>.ext</td><td>.ext indicates file extension type:
<table>
<tr><th>File Extension</th><th>Description</th></tr>
<tr><td>.jpg</td><td>Browse images of the Northern and Southern Hemispheres</td></tr>
<tr><td>.HDFEOS</td><td>Data file in HDF-EOS format</td></tr>
<tr><td>.xml</td><td>Granule metadata file in Extensible Markup Language (XML)</td></tr>
</table></td></tr>
</table>

Example File Names:

```
NISE_SSMISF18_20161223.1.jpg
NISE_SSMISF18_20161223.2.jpg
```

```
NISE_SSMISF18_20161223.HDFEOS
NISE_SSMISF18_20161223.HDFEOS.xml
```

1.3 Spatial Information

1.3.1 Coverage

Spatial coverage is global except for a gap of three degrees latitude (87 to 90 degrees) from each pole. The application of monthly-varying masks limits the mapped extent of snow and sea ice in both hemispheres (see the Data Acquisition and Processing section of this document for more details). Spatial coverage is shown in Figure 3 and Figure 4.

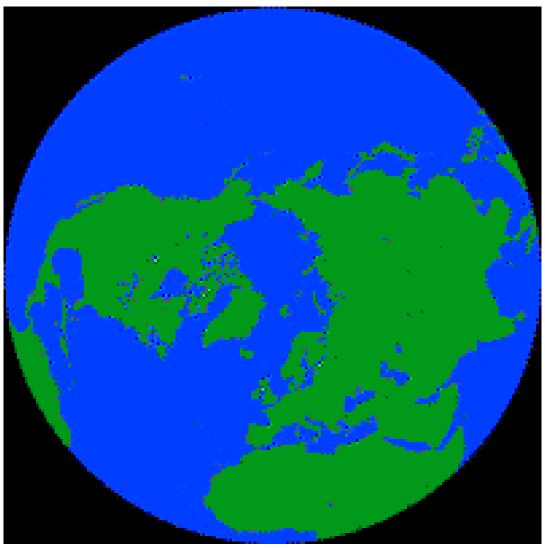

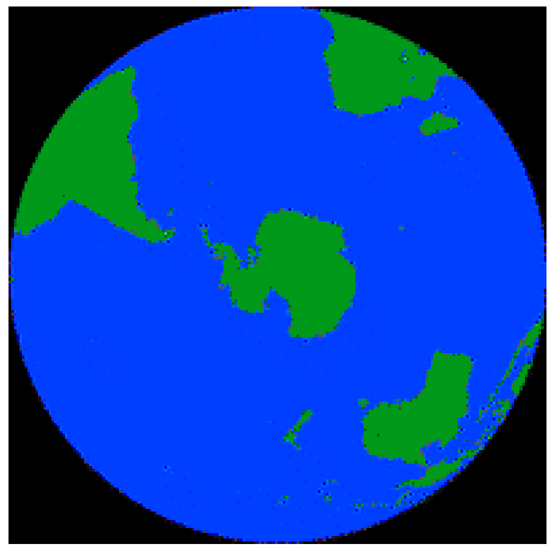

1.3.2 Resolution

The polar EASE grids have a nominal resolution of 25 km.

1.3.3 Geolocation

Sea ice concentration and snow extent maps are provided in the 25 km Northern Hemisphere and Southern Hemisphere Equal-Area Scalable Earth Grids (EASE-Grid North and EASE-Grid South). Table 3 and Table 4 below provide more details.

Table 3. Geolocation Details

Geographic coordinate system	Unspecified datum based upon the International 1924 Authalic Sphere	Unspecified datum based upon the International 1924 Authalic Sphere
Projected coordinate system	NSIDC EASE-Grid North	NSIDC EASE-Grid South
Longitude of true origin	0	0
Latitude of true origin	90	-90
Scale factor at longitude of true origin	N/A	N/A
Datum	Not specified based on the International 1924 Authalic Sphere	Not specified based on the International 1924 Authalic Sphere
Ellipsoid/spheroid	International 1924 Authalic Sphere	International 1924 Authalic Sphere
Units	meter	meter
False easting	0	0
False northing	0	0
EPSG code	3408	3409
PROJ4 string	+proj=laea +lat_0=90 +lon_0=0 +x_0=0 +y_0=0 +a=6371228 +b=6371228 +units=m +no_defs	+proj=laea +lat_0=-90 +lon_0=0 +x_0=0 +y_0=0 +a=6371228 +b=6371228 +units=m +no_defs
Reference	http://epsg.io/3408	http://epsg.io/3409

Table 4. Grid Details

Projection Coordinate System	NSIDC EASE-Grid North	NSIDC EASE-Grid South
Grid cell size (x, y pixel dimensions)	25,067.53 m x 25,067.53 m	25,067.53 m x 25,067.53 m
Number of rows	721	721
Number of columns	721	721
Geolocated lower left point in grid	N/A, off the Earth	N/A, off the Earth
Nominal gridded resolution	25 km	25 km
Grid rotation	none	none
ulxmap – x-axis map coordinate of the center of the upper-left pixel (XLLCORNER for ASCII data)	-9036842.76	-9036842.76
ulymap – y-axis map coordinate of the center of the upper-left pixel (YLLCORNER for ASCII data)	9036842.76	9036842.76

1.4 Temporal Information

1.4.1 Coverage

Data coverage begins on 09 July 1987 and is ongoing. Table 5 lists the temporal coverage by data set version (i.e., by satellite).

Table 5. Temporal Coverage

NISE Version	DMSP Platform	Sensor	Temporal Coverage
2	F13	SSM/I	1995-05-04 to 2009-09-11
3	F16	SSMIS	2012-01-01 to present
4	F17	SSMIS	2009-08-17 to present
5	F18	SSMIS	2016-12-01 to present

1.4.2 Resolution

Data are available at a daily resolution.

For each 24-hour period, NISE is updated using the most recent input data for a given grid cell. The frequency of input updates varies as a function of latitude. Grid cells representing latitudes above 55° N or below 55° S, for which multiple satellite passes are available each day, are usually updated every 24 hours. Due to the orbital geometry of the DMSP satellites and the swath width of the SSM/I and SSMIS sensors, the time interval between successive observations at low-latitude locations (20° S to 20° N) can be up to five days (Hollinger et al. 1987). Given the absence of sea ice and very limited snow extent at these low latitudes, the infrequent updates were deemed acceptable.

Occasionally, input data are unavailable or unobtainable. When this happens, the age values at any location may be older than five days. An age grid indicates the number of days since each grid cell was last updated.

2 DATA ACQUISITION AND PROCESSING

2.1 Background

NSIDC modified the snow extent mapping algorithm in March 2002, based primarily on a study by Armstrong and Brodzik (2002). This study indicated that horizontal-polarization-based algorithms underestimate snow extent during early winter but provide the best overall estimates of snow extent at the continental to hemispheric scale through the period of maximum snow extent and into the melt season. Vertical-polarization-based algorithms (Goodison, 1989) provide similar results but with a consistent tendency to falsely identify snow-free desert soils and/or frozen ground as snow-covered.

2.2 Instrumentation

Beginning in 1987, a series of satellites was launched by the Defense Meteorological Satellite Program (DMSP) carrying sensors designed to provide global passive microwave data in support of the United States' military, commercial, and scientific operations. The Special Sensor Microwave Imager (SSM/I) instrument is a seven-channel, four-frequency, orthogonally polarized, passive microwave radiometric system. The instrument measures combined atmosphere and surface radiances at 19.3 GHz, 22.2 GHz, 37.0 GHz, and 85.5 GHz frequencies. Horizontal and vertical polarization measurements are available.

The Special Sensor Microwave Imager/Sounder (SSMIS) instrument is the next generation Special Sensor Microwave/Imager (SSM/I) instrument. It is a conically-scanning passive microwave radiometer that harnesses the imaging capabilities of SSM/I (with coincident channels except that 91.7 GHz replaces 85.5 GHz) and the sounding capabilities of the DMSP SSM/T-1 temperature and SSM/T-2 water vapor sounders. The SSMIS sensor has a swath width of 1700 km.

Refer to the SMMR, SSM/I, and SSMIS Sensors Summary for more details.

2.3 Acquisition

The NISE Versions 3, 4, and 5 products use passive microwave data from the SSMIS onboard the DMSP-F16, -F17, and -F18 satellites, respectively. The NISE Version 2 product uses passive microwave data from the SSM/I onboard the DMSP-F13 satellite.

Table 6. Input Data Sources

NISE Version	Sensor	Satellite
5	Special Sensor Microwave Imager/Sounder (SSMIS)	DMSP-F18
4	Special Sensor Microwave Imager/Sounder (SSMIS)	DMSP-F17
3	Special Sensor Microwave Imager/Sounder (SSMIS)	DMSP-F16
2	Special Sensor Microwave Imager (SSM/I)	DMSP-F13
1	N/A, no product available	

2.4 Processing

The process to derive snow extent from passive microwave satellite data is constantly undergoing revision and improvement at NSIDC. All algorithms are subject to change without warning. Changes are intended to improve the snow and ice mapping capabilities of NSIDC.

Sea ice concentrations are derived from all SSM/I or SSMIS data from a given 24-hour period, binned to the EASE-Grid using a "drop-in-the-bucket" interpolation method. Derivations use the NASA Team Sea Ice (first-year ice plus multi-year ice) Algorithm, as described in Cavalieri et al. (1992). For more details on the algorithm, see the Descriptions of and Differences between the NASA Team and Bootstrap Algorithm FAQ.

Snow extent is also derived from passive microwave satellite data. Snow extent is mapped using an algorithm developed for Scanning Multichannel Microwave Radiometer (SMMR) data, as described in Chang, Foster, and Hall (1987), and modified for use with SSM/I and SSMIS data, as described in Armstrong and Brodzik (2001). Snow extent derivations use Brightness Temperature (Tb) measurements from the satellite's morning pass as inputs and rely on nearest neighbor interpolation.

A land/ocean/ice cap mask is used to determine which interpolation algorithm (sea ice concentration or snow extent) is used for each pixel. Additional climatology masks are used to identify spurious data, primarily due to weather affecting passive microwave data collection. Currently, the sea ice climatology is a monthly ocean mask derived from historical SMMR (1979-1987) and SSM/I (1987-2003) data. The snow extent climatology for the Northern Hemisphere is a monthly mask derived from the Northern Hemisphere EASE-Grid Weekly Snow Cover and Sea Ice Extent (October 1966 to May 2005) data. The original Southern Hemisphere snow climatology was a static file that served as a spatial representation of the expected snow line in the Andes, relying on a function of latitude and elevation to determine snow extent (Schwerdtfeger, 1976); NISE files dated before 30 June 2005 use the original mask. Beginning 01 July 2005, the snow extent climatology for the Southern Hemisphere is a monthly mask derived from SSM/I period (1987 to 2003) data.

2.5 Quality, Errors, and Limitations

2.5.1 Quality Control

NSIDC periodically performs visual inspections of daily browse images.

As part of the public release of all versions in February 2021, NSIDC examined differences between hemispheric fields generated from F16, F17 and F18—versions 3, 4, and 5 respectively—by comparing daily total extents of both sea ice and snow-covered areas.

Small inconsistencies are expected between sensors. This analysis showed overall consistency between F16 and F17, but it uncovered increasing differences between Northern Hemisphere total snow-covered area calculated from F16(v3) and F18(v5), as well as F17 (v4) and F18 (v5) (Figure 5). In Figure 6, we show an example of particularly large differences to illustrate their spatial patterns. In this example, a few large areas of disagreement stand out (e.g. the North American Great Plains and in the Ontario region), but otherwise the disagreements happen mostly along the edges of the snow extent.

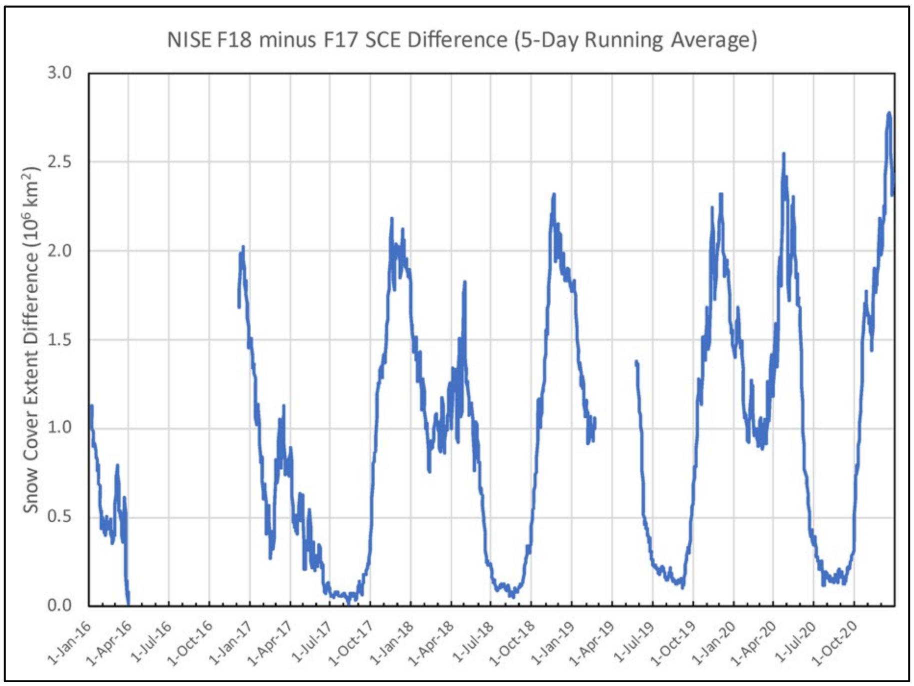

Figure 5. Time-series showing the 5-day moving average of the difference between snow-covered areas given by F18 and F17.

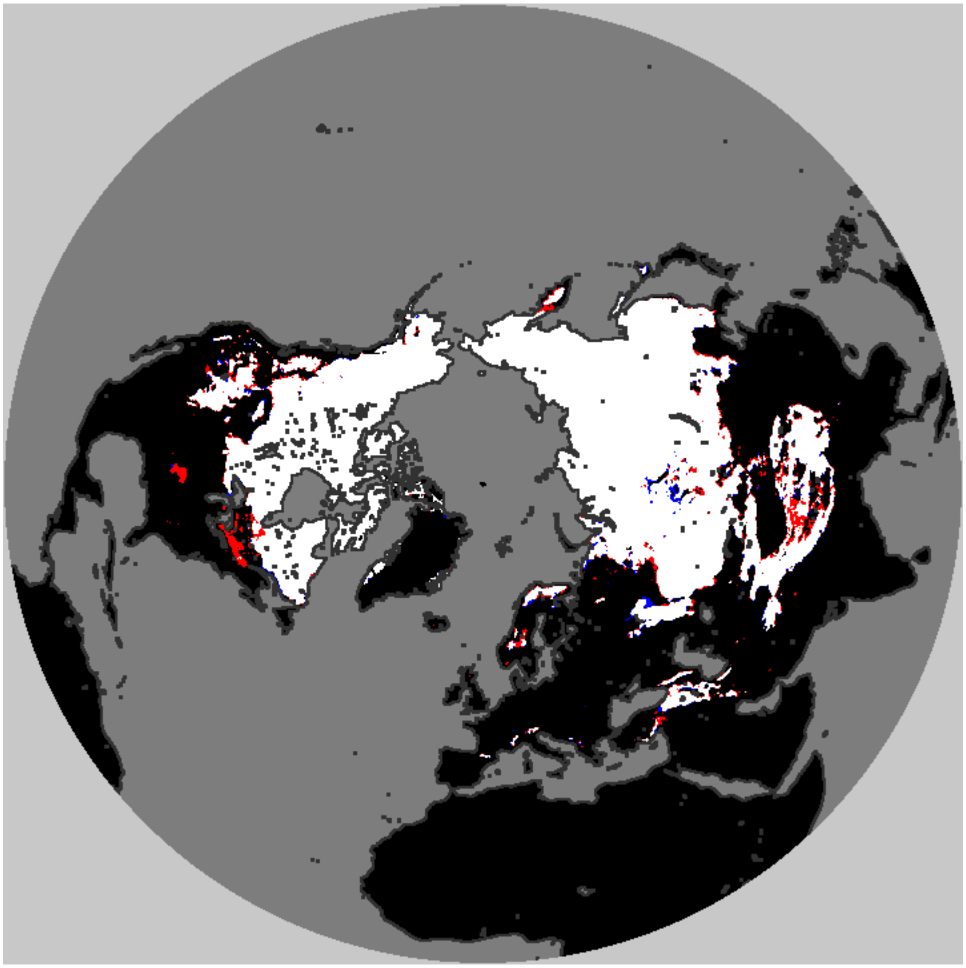

Figure 6. Map illustrating where F17 and F18 agree and disagree for 12 March 2020, as an example of their spatial differences. Areas in black are free of snow in both F17 and F18; areas in blue have snow only in F17; areas in red have snow only in F18; and areas in white have snow in both F17 and F18.

Because of these differences, NSIDC implemented updated coefficients for the NISE snow algorithm for F16 and F18 so that the snow-covered area calculations for these sensors better matched the snow-covered area calculated from F17 observations. These updated coefficients were derived by (1) calculating monthly masks where snow extent was found in any of the F16, F17, and F18 fields during calendar years 2019 and 2020, (2) computing a linear regression between the brightness temperatures of F16 and F18 versus F17 where coincident observations were available, (3) computing updated SCA coefficients using these relationships, and finally (4) searching for small changes in these coefficients which yielded a lower absolute value of SCA extent when compared to F17 fields. Summary statistics of the average difference and standard deviation of the difference for 2019 and 2020 are listed in Table 7, where “old” refers to data with the previous coefficients and “new” refers to data with the adjusted coefficients. Figures 7-10 illustrate differences in snow extent by area and percentage among F16 old and new, F17, and F18 old and new sensors.

Table 7. Differences in total NISE snow cover extent between estimates from SSMIS on F18/16 Old/New coefficients and F17 (units of 10^6 km^2).

	F 18 Old – F17	F18 New – F17	F16 Old – F17	F16 New – F17
2019 Average	1.12	0.01	0.75	0.01
2020 Average	1.23	0.10	0.75	0.03
2019 St. Dev.	0.67	0.48	0.54	0.59
2020 St. Dev.	0.73	0.54	0.50	0.52

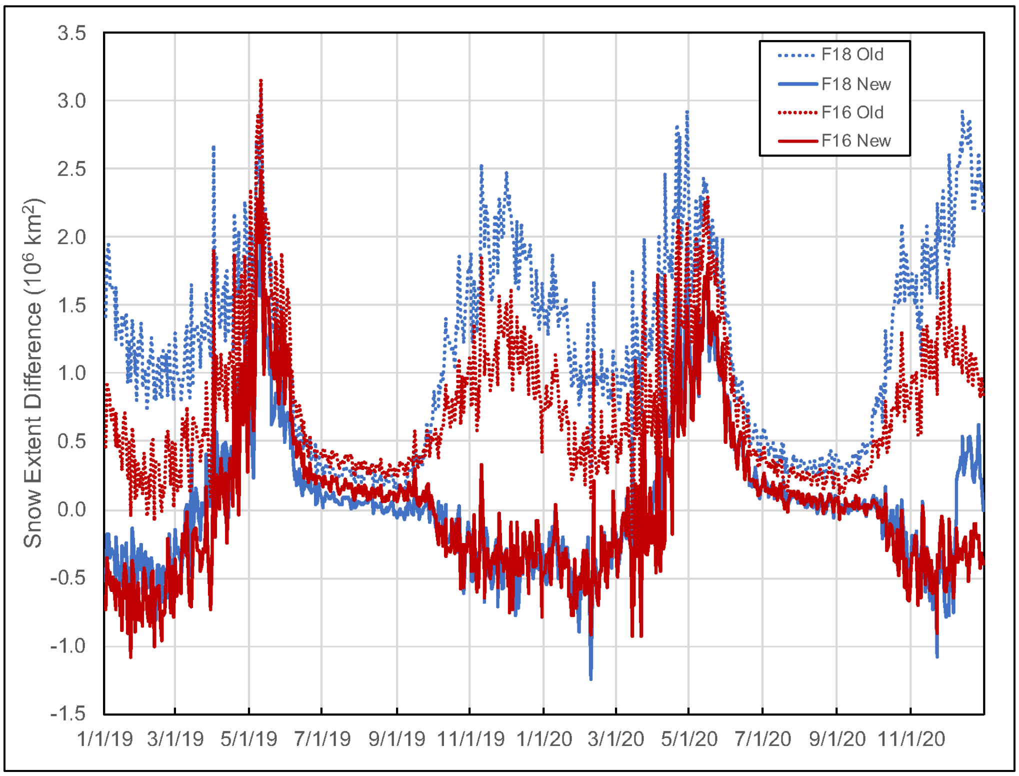

Figure 7. Snow extent difference in km^2 between F18 and F16 sensors.

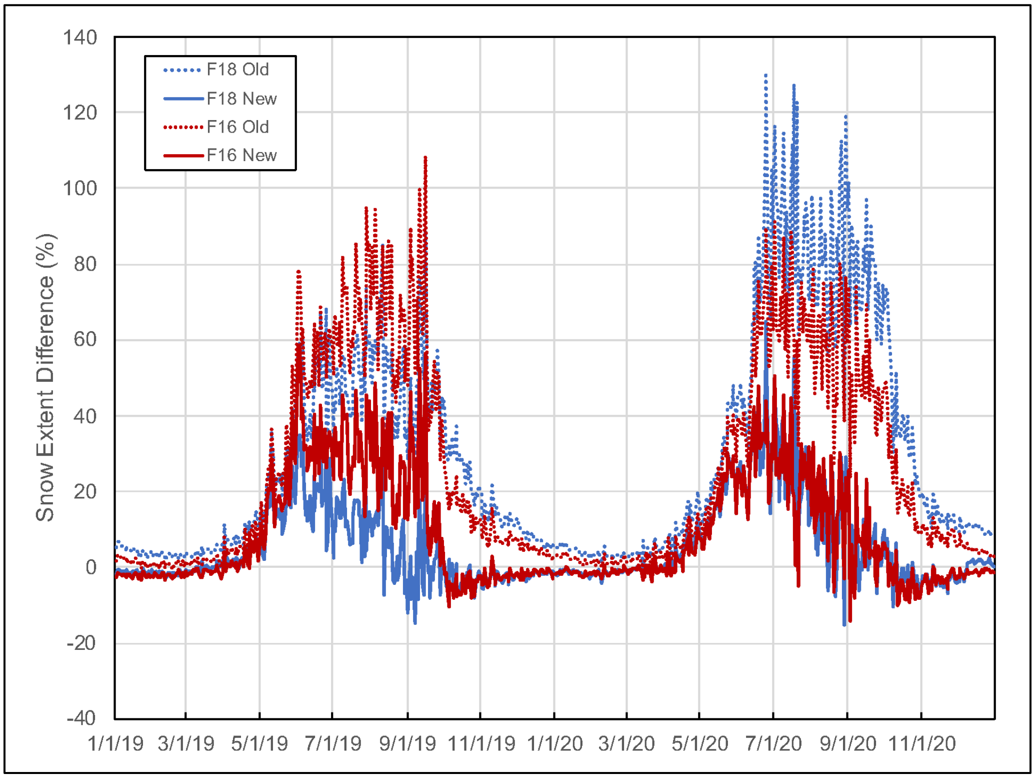

Figure 8. Snow extent difference by percentage between F18 and F16 sensors.

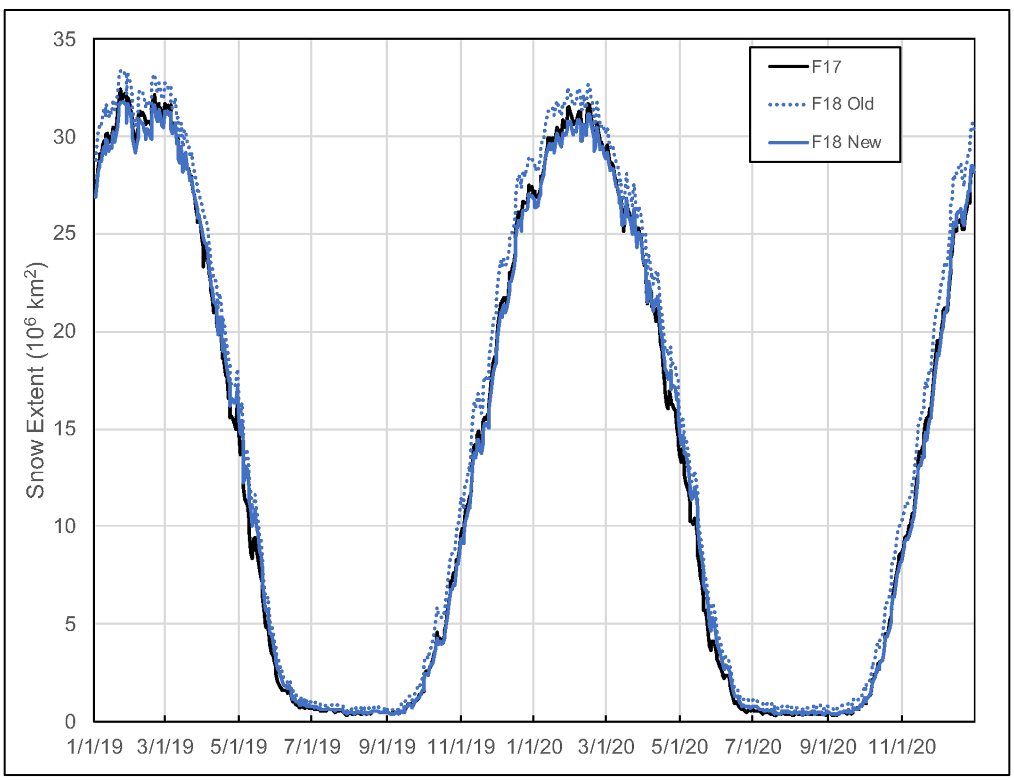

Figure 9. Snow extent difference in km^2 between F17 and F18 sensors.

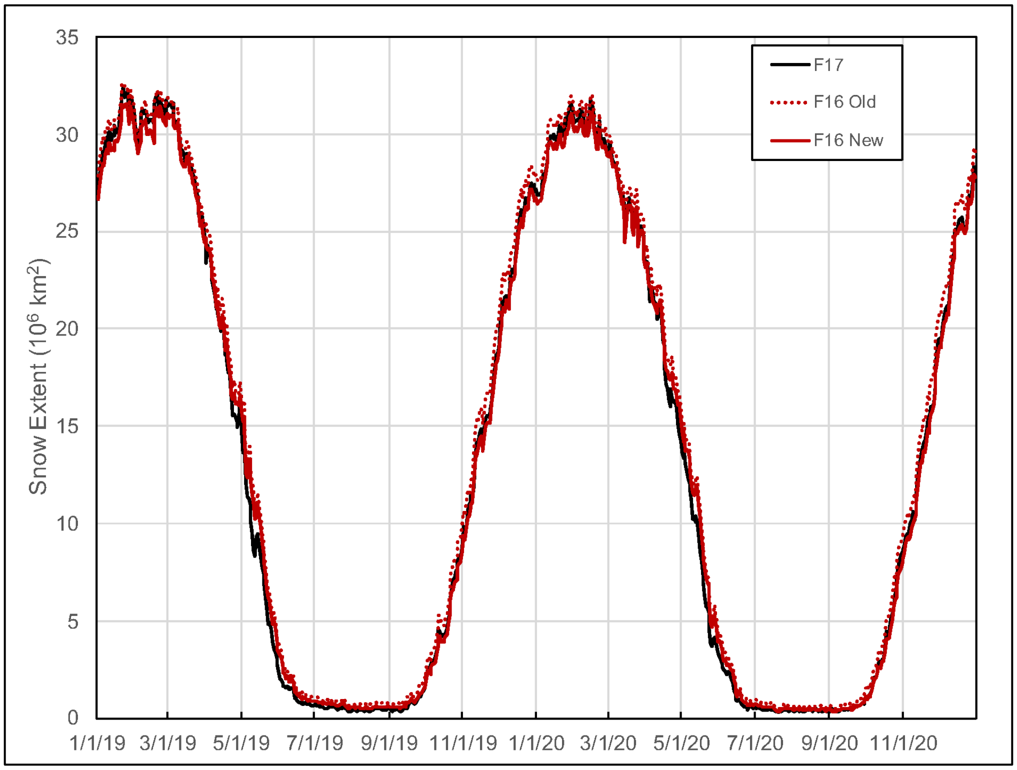

Figure 10. Snow extent difference in km^2 between F17 and F16 sensors.

Differences in sea ice areas between the sensors are small and not very noticeable, so no adjustments are needed.

2.5.2 Error Sources

Physical conditions affecting the accuracy of the sea ice concentration algorithm include atmospheric water content, ocean roughening and spray, presence of thin ice, and formation of melt ponds on the sea ice. Errors become greatest during mid- to late-summer, resulting primarily from melt ponds on the ice surface, and also from atmospheric- and weather-related effects over open ocean. To minimize the error over open ocean, a filter is applied to detect these atmospheric effects. False ice concentration estimates may also occur along coastlines due to mixed pixels. Mixed pixels contain signals from both land and water in unknown proportions. For the NISE product, such errors are minimized by designating these pixels as coastal pixels (see Table 1 for more details).

The presence of dense coniferous and deciduous forests presents problems for mapping snow extent because the vegetation canopy obscures snow on the ground. The best conditions for accurate snow extent mapping are in areas of little or no vegetation, such as prairies and tundra. In all areas, the snow extent mapping algorithm only identifies a grid cell as snow-covered when it has a computed snow depth greater than 2.5 cm.

Known problems with SSM/I and SSMIS data include occasional missing data, poor quality scan lines, and out-of-bounds data values. Such errors usually result in no new NISE observations at affected locations on those days, so the most recent prior observation at that location is used instead. The age field indicates when the pixel's latest observation was made.

Errors may also be introduced when the T_b data that the sea ice concentration and snow extent algorithms use become unreliable. For instance, on 5 April 2016 a solar panel on board the DMSP F-17 satellite changed position, and the integrity of the vertically polarized 37 GHz channel (37V) channel of the SSMIS sensor was affected. Since this is one of the primary channels used in the NISE processing, NISE Version 4 data from this time onward should be used with caution. Largely as a result of this incident, NISE began using data from DMSP-F18 on 1 November 2016 (start of Version 5) and from DMSP-F16 on 1 January 2012 (start of Version 3).

2.5.3 Confidence Level/Accuracy Judgment

Sea ice concentration estimates are accurate to within approximately 5% in most areas for the most of the year. Armstrong and Brodzik (2001) demonstrated that the snow extent algorithm can provide daily global snow extent maps with an accuracy of approximately 50 km, except in areas of wet snow or dense forest cover. When the snow is wet – when liquid water is present on the snow grain surface – the snow pack becomes predominantly an emitter and much of the scattered portion of the ground signal is lost, greatly limiting algorithm accuracy. To reduce the frequency of observations over wet snow, only data from the early morning (descending) orbits are used as input to the algorithm.

NSIDC performed inter-calibration between F17 and F18 data (NISE Version 4 and NISE Version 5) and found that the sea ice algorithm coefficients yield similar ice extents during an overlap period between 01 March 2015 and 29 February 2016. Thus, F18 sea ice estimates should be reasonably consistent with F17 estimates, although differences of up to approximately 28,000 km^2 may be possible in daily total extents. The differences are primarily near the ice edge, where shifts of one to two grid cells (25-50 km) may be seen.

Version 5 of NISE incorporates a spillover correction (Cavalieri et al., 1999) that reduces or eliminates sea ice concentrations near coastlines when there is open water present. Due to the relatively large microwave footprint size, passive microwave emissions from adjacent land masses contaminate the signal for coastal pixels, producing spurious sea ice extents in coastal regions that are actually void of sea ice, especially during summer months.

2.5.4 Applications and Limitations

This data set was originally designed to provide NASA EOS researchers with near-real-time daily, global snow extent and sea ice concentration data. The following NASA EOS instrument teams use the NISE data to generate their products:

- Multi-angle Imaging SpectroRadiometer (MISR). The MISR instrument is part of a suite of sensors on NASA's EOS Terra satellite. The NISE product will be used as ancillary data for the MISR Top-of-Atmosphere/Cloud product, which requires near-real-time daily, global snow and sea ice extent data.

- Clouds and the Earth's Radiant Energy System (CERES). CERES requires both daily and monthly averaged global snow and ice extent maps for several of their Earth radiation budget products. CERES is currently part of the Tropical Rainfall Measuring Mission (TRMM) aboard the EOS Terra platform.

- Moderate Resolution Imaging Spectroradiometer (MODIS). The MODIS Atmosphere Discipline Group uses NISE data to produce their cloud mask.

NSIDC anticipates additional use of the NISE product to:

- Produce sea surface temperature maps from the MODIS instrument.

- Provide ancillary data to the Global Land Ice Monitoring from Space project, which uses the Advanced Spaceborne Thermal Emission and Reflection Radiometer (ASTER).

- Compare with Advanced Microwave Scanning Radiometer (AMSR) sea ice concentrations and snow extent maps.

3 SOFTWARE AND TOOLS

The EASE Grid Data Tools page provides files containing latitude and longitude values for each EASE-Grid North and EASE-Grid South grid cell. Fortran and C source code are also available for converting grid cell locations to latitude and longitude values, and vice-versa. An Interactive Data Language (IDL) program is available for converting latitude and longitude values to grid column and row coordinates.

The NSIDC Hierarchical Data Format - Earth Observing System (HDF-EOS) web site provides information about the HDF-EOS format, tools that extract HDF-EOS objects into ASCII or flat binary formats, and links to other HDF-EOS resources. In addition, example code for access and visualization of NISE data in NCL, Matlab, and IDL is provided on the HDF-EOS Comprehensive Examples page.

4 VERSION HISTORY

Table 8. Description of Significant Revisions

Version	Implementation date (yyyy-mm-dd)	Description
V5.1	2021-08-16	The coefficients for the F18 NISE snow algorithm were updated to better match F17 SCA extents.
V3.1	2021-08-16	The coefficients for the F16 NISE snow algorithm were updated to better match F17 SCA extents.
V5	2016-12-02	The NISE snow and sea ice algorithms both use near-real-time brightness temperature observations from the SSMIS instrument on DMSP-F18. The coefficients for the NISE snow algorithm were updated to better match results from DMSP-F13 as a result of an inter-calibration between F13 and F17 during an overlap period from 3/27/2008-3/26/2009 and between F17 and F18 during an overlap period from 7/1/2014-6/30/2015. ESDT metadata was updated to reflect the change in the data set version. The NISE Version 5 data record begins 12/01/2016. A two-month overlap with NISE Version 4 is planned: 12/01/2016-01/31/2017
V4.1	2009-10-12	Updated metadata field values for PGEVERSION (collection level remains Version 4) Removed 15% sea ice concentration threshold that assigned pixels with a sea ice concentration of <15% as ocean (data value of 255) Reprocessed NISE Version 4 to include sea ice concentration values of 1-14% This revision is an update to NISE Version 4. All Version 4 data (17 August 2009 - present) have been reprocessed with this system.

Version	Implementation date (yyyy-mm-dd)	Description
V4	2009-08-28	Changed input processing stream from the SSM/I instrument on board the DMSP-F13 satellite to the SSMIS instrument on DMSP-F17 Changed input processing stream from NASA GHRC to NOAA CLASS Conducted inter-calibration between F13 and F17 to correct for sensor differences using an overlap period of 28 March 2008 - 28 March 2009; adjusted tie points for the sea ice component of NISE; adjusted the snow extent algorithm component of NISE. Updated metadata field values for VERSIONID, LOCALVERSIONID and PGEVERSION Changed definition of one day from orbit boundaries to UTC time; thus, changed algorithm to determine one day of input data using midnight to midnight UTC, rather than orbit boundaries. Previous versions of NISE determined the beginning of a day with the first complete orbit past midnight, and completed the day with the last orbit prior to midnight. Implemented a land-to-ocean spillover correction to reduce spurious ice near shorelines (Cavalieri et al., 1999) This revision is designated NISE Version 4. All data from 17 August 2009 to the present have been processed with this system. The NISE Version 2 product from F13 has been produced through 31 August 2009. (No NISE Version 3 product was available at the time).
V3	2021-02-04	Data release using SSMIS DMSP-F16 input data stream.
V2.3	2008-10-06	Ported NISE processing system from SGI to linux. No significant changes in output.
V2.2	2006-04-27	New Northern Hemisphere snow climatologies with data from 1966-2005, and new Northern and Southern Hemisphere ice climatologies with data from 1979-2003.
V2.1	2005-07-01	Static Southern Hemisphere snow climatology limiting possible snow to the Andes region was replaced with a monthly climatology that now includes the Andes and New Zealand.
V2	2005-06-10	Data from the start of the SSM/I F13 mission (04 May 1995) to 31 December 1999 were processed to NISE Version 2.

Version	Implementation date (yyyy-mm-dd)	Description
V1.11	2005-04-25	A new LOCI mask was used, based on the Boston University (BU)-MODIS land cover data set Updated HDF libraries from HDF 4.1r1 to 4.1r3 Updated metadata field values for VERSIONID, LOCALVERSIONID and PGEVERSION Corrected error in browse images that was painting pixels blue at the edge of the snow pack This revision is designated NISE Version 2. All data from 01 January 2000 to present have been reprocessed with this system. NISE Version 1 files will be deleted at a future date.
V1.10	2003-09-25	New, improved LOCI (land-ocean-coastline-ice) masks Brightness temperature interpolation method for land areas (snow algorithm) changed from nearest neighbor to inverse distance squared.
V1.9	2002-03-20	New snow extent algorithm
V1.8	2000-06-01	New ice climatologies through 1999
V1.7	2000-03-02	Changed metadata field for PRODUCTIONDATETIME from local time to UTC
V1.6	2000-01-07	Second modifications for managing data in the EOSDIS Core System (ECS) Reprocessed files beginning with 1999-12-29 to be Y2K compatible Created HDF browse file Added metadata to HDF-EOS files, starting with 1999-12-29
V1.5	1999-10-07	First modifications for managing data in the EOSDIS Core System (ECS)
V1.4	1999-04-09	Fixed geolocation errors in NISE-to-HDFEOS program
V1.3	1998-08-06	New ice climatologies developed at NSIDC that use SMMR data from 1979-87 and SSM/I data through 1996 New land-ocean-coastlines-ice (LOCI) masks that fix isolated coastline pixel problems
V1.2	1998-02-01	New ice climatologies developed at NSIDC instead of GSFC New Southern Hemisphere snow climatologies derived from altitude and latitude freeze-line information
V1.1	1997-12-31	Fixed 2-digit year problem in time for new year
V1	1997-10-31	Initial operational release

5 RELATED DATA SETS

Sea Ice Products

Sea Ice Data at NSIDC

Snow Extent Data at NSIDC

MODIS Snow Cover Data at NSIDC

6 CONTACTS AND ACKNOWLEDGMENTS

Mary Jo Brodzik
National Snow and Ice Data Center
University of Colorado
Boulder, Colorado USA

J. Scott Stewart
National Snow and Ice Data Center
University of Colorado
Boulder, Colorado USA

Acknowledgments:
NASA provided funding for the production of this data set through the NSIDC Distributed Active Archive Center (DAAC).

7 REFERENCES

Armstrong, R. L. and M. J. Brodzik. 2001. Recent Northern Hemisphere Snow Extent: A Comparison of Data Derived from Visible and Microwave Satellite Sensors. *Geophysical Research Letters*, 28(19): 3673-3676. https://doi.org/10.1029/2000GL012556

Armstrong, R. L. and M. J. Brodzik. 2002. Hemispheric-Scale Comparison and Evaluation of Passive-Microwave Snow Algorithms. *Annals of Glaciology*, 34: 38-44. https://doi.org/10.3189/172756402781817428

Cavalieri, D. J., C. l. Parkinson, P. Gloersen, J. C. Comiso, and H. J. Zwally. 1999. Deriving Long-Term Time Series of Sea Ice Cover from Satellite Passive-Microwave Multisensor Data Sets. *Journal of Geophysical Research*, 104(7): 15,803-15, 814. https://doi.org/10.1029/1999JC900081

Cavalieri, D. J., J. Crawford, M. Drinkwater, W. J. Emery, D. T. Eppler, L. D. Farmer, M. Goodberlet, R. Jentz, A. Milman, C. Morris, R. Onstott, A. Schweiger, R. Shuchman, K. Steffen, C. T. Swift, C. Wackerman, and R. L. Weaver. 1992. *NASA Sea Ice Validation Program for the DMSP*

SSM/I: Final Report. NASA Technical Memorandum 104559. National Aeronautics and Space Administration, Washington, D. C. 126 pages.

Chang, A. T. C., J. L. Foster, and D. K. Hall. 1987. Nimbus-7 SMMR Derived Global Snow Cover Parameters. *Annals of Glaciology*,9: 39-44. https://doi.org/10.3189/S0260305500200736

Goodison, B. E. 1989. Determination of Areal Snow Water Equivalent on the Canadian Prairies Using Passive Microwave Satellite Data. *IGARRS '89 Proceedings*, 3:1243-6. https://doi.org/10.1109/IGARSS.1989.576061

Hollinger, J. P., R. C. Lo, G. A. Poe, R. Savage, and J. L. Peirce, 1987. *Special Sensor Microwave/Imager User's Guide*. Washington, D.C.: Naval Research Laboratory.

Schwerdtfeger, W. 1976. *Climate of Central and South America*. World Survey of Climatology 12. New York: Elsevier Scientific Publishing. https://doi.org/10.1002/qj.49710343520

8 DOCUMENT INFORMATION

8.1 Original Publication Date

November 2019

8.2 Date Last Updated

December 2021